UNIVERSITY OF LEEDS

This is a repository copy of *Cadmium Isotope Fractionation during Adsorption and Substitution with Iron (Oxyhydr)oxides*.

White Rose Research Online URL for this paper:
https://eprints.whiterose.ac.uk/177162/

Version: Accepted Version

Article:
Yan, X, Zhu, M, Li, W et al. (7 more authors) (2021) Cadmium Isotope Fractionation during Adsorption and Substitution with Iron (Oxyhydr)oxides. Environmental science & technology. ISSN 0013-936X

https://doi.org/10.1021/acs.est.0c06927

Reuse
Items deposited in White Rose Research Online are protected by copyright, with all rights reserved unless indicated otherwise. They may be downloaded and/or printed for private study, or other acts as permitted by national copyright laws. The publisher or other rights holders may allow further reproduction and re-use of the full text version. This is indicated by the licence information on the White Rose Research Online record for the item.

Takedown
If you consider content in White Rose Research Online to be in breach of UK law, please notify us by emailing eprints@whiterose.ac.uk including the URL of the record and the reason for the withdrawal request.

White Rose university consortium
Universities of Leeds, Sheffield & York

eprints@whiterose.ac.uk
https://eprints.whiterose.ac.uk/

Cadmium Isotope Fractionation during Adsorption and Substitution with Iron (Oxyhydr)oxides

Xinran Yan[1,2], Mengqiang Zhu[3], Wei Li[4], Caroline L. Peacock[5], Jingyuan Ma[6], Hanjie Wen[7], Fan Liu[1,2], Zhengbing Zhou[8], Chuanwei Zhu[7,*], Hui Yin[1,2,*]

[1]Key Laboratory of Arable Land Conservation (Middle and Lower Reaches of Yangtse River), Ministry of Agriculture and Rural affairs, College of Resources and Environment, Huazhong Agricultural University, Wuhan 430070, China.

[2]State Environmental Protection Key Laboratory of Soil Health and Green Remediation, Ministry of Ecology and Environment, Huazhong Agricultural University, Wuhan 430070, China.

[3]Department of Ecosystem Science and Management, University of Wyoming, 1000 E. University Ave., Laramie, WY 82071, USA

[4]Key Laboratory of Surficial Geochemistry, Ministry of Education, School of Earth Sciences and Engineering, Nanjing University, Nanjing 210023, China

[5]School of Earth and Environment, University of Leeds, Leeds, LS2 9JT, UK

[6]Shanghai Synchrotron Radiation Facility, Shanghai Institute of Applied Physics, Chinese Academy of Sciences, Shanghai 201204, China

[7]State Key Laboratory of Ore Deposit Geochemistry, Institute of Geochemistry, Chinese Academy of Sciences, Guiyang 550002, China

[8]State Key Laboratory of Nuclear Resources and Environment, East China University of Technology, Nanchang, 330013, China

Corresponding Authors:

Tel.: +86 27 87280271. Fax: +86 27 87288618.

Email: yinhui666@mail.hzau.edu.cn; zhuchuanwei@mail.gyig.ac.cn.

ABSTRACT: Cadmium (Cd) isotopes have great potentials for understanding Cd geochemical cycling in soil and aquatic systems. Iron (oxyhydr)oxides can sequester Cd via adsorption and isomorphous substitution, but how these interactions affect Cd isotope fractionation remains unknown. Here we show that adsorption preferentially enriches lighter Cd isotopes on iron (oxyhydr)oxide surfaces through equilibrium fractionation, with similar fractionation magnitudes ($\Delta^{114/110}Cd_{solid\text{-}solution}$) for goethite (-0.51 ± 0.04‰), hematite (-0.54 ± 0.10‰) and ferrihydrite (-0.55 ± 0.03‰). Neither initial Cd^{2+} concentration, ionic strength nor pH influence the fractionation magnitudes. The enrichment of the light isotope is attributed to the adsorption of highly distorted [CdO_6] on solids as indicated by Cd K-edge EXAFS analysis. In contrast, Cd incorporation into goethite by substitution for lattice Fe at a Cd/Fe molar ratio of 0.05 preferentially sequesters heavy Cd isotopes, with $\Delta^{114/110}Cd_{solid\text{-}solution}$ of 0.22 ± 0.01‰. The fractionation probably occurs during the transformation of ferrihydrite to goethite via dissolution and reprecipitation. These results improve the understanding of Cd isotope fractionation behavior affected by iron (oxyhydr)oxides in Earth's critical zone, and demonstrate that interactions with minerals can obscure anthropogenic and natural Cd isotope characteristics, which should be carefully considered when applying Cd isotopes as environmental tracers.

KEYWORDS: Metal (oxyhydr)oxides, Heavy metal isotopes, Adsorption, Coprecipitation, Mineral transformation, Extended X-ray absorption fine structure spectroscopy

SYNOPSIS

The widespread iron (oxyhydr)oxides in Earth's critical zone play an important role in Cd isotope fractionation behaviors.

INTRODUCTION

Cadmium (Cd) is a highly toxic and carcinogenic heavy metal for humans without a safe exposure limit.[1-3] Risk prediction and remediation of anthropogenic Cd pollution in terrestrial environments requires a fundamental understanding of its geochemical cycling. Recently, Cd isotope signatures have been increasingly applied to understand biogeochemical reactions and fingerprint Cd sources and fate in contaminated ecosystems.[4-9] However, this promise is hampered as multiple processes can cause heavy metal isotope fractionation, such as adsorption onto mineral surfaces,[9,10] coprecipitation with minerals,[11,12] complexation by inorganic[13] or organic ligands[14,15], membrane protein transport in plants[16] and weathering[9,17]. Among these processes, adsorption and coprecipitation on mineral surfaces or structural incorporation into mineral lattices are of much importance, which are the well-known association mechanisms of heavy metals with minerals, particularly for Cd, Zn and Ni.[10,18-30]

Metal isotope fractionation during adsorption onto mineral surfaces can be affected by mineral phases, pH, ionic strength (IS), surface loading and reaction time. Following an equilibrium isotope fractionation, Zn adsorbed on Fe (oxyhydr)oxides is enriched in heavy isotopes; and the fractionation magnitude on ferrihydrite is stronger than that on goethite.[20] In synthetic seawater, birnessite (a Mn oxide) also retains heavy Zn isotopes, with the fractionation magnitude decreasing with increasing surface loading or decreasing IS.[31] Light Ni isotopes are preferentially adsorbed onto Fe (oxyhydr)oxides with the fractionation magnitude on goethite much larger than that on

93 ferrihydrite.[19,21] Finally for Cd, birnessite was reported to preferentially adsorb light Cd
94 isotopes, with the fractionation magnitude increasing with increasing IS but decreasing
95 with reaction time.[10]

96 Metal incorporation into the mineral structure can also induce isotope fractionation,
97 generally following a kinetic fractionation mechanism. Incorporation of Zn into the
98 calcite lattice during coprecipitation preferentially enriches heavy isotopes.[32]
99 Additionally, the isotope fractionations of metal may behave inversely when interacting
100 with different minerals. Heavy Ni isotopes incorporate into birnessite layers as a result
101 of adsorption at pH 8.2,[22] however, its coprecipitation with ferrihydrite shows
102 indistinguishable fractionations from that caused by adsorption, i.e., enriching light
103 isotopes in the solids[19]. During Cd precipitation with sulfur (S), light Cd isotopes are
104 sequestered in CdS.[12] Substitution of Cd for calcite lattice Ca during the crystal growth
105 in freshwater does not lead to Cd isotope fractionation, but in artificial seawater light
106 Cd isotopes are enriched in solid.[11,33,34]

107 According to the isotope fractionation theory,[35] heavy isotopes tend to be
108 concentrated in chemical species forming the stiffest bonds with short bond lengths.
109 Heavier Zn isotopes in [ZnO_4] compared to [ZnO_6] during Zn adsorption onto Fe/Mn
110 (oxyhydr)oxides can be well explained by the substantially shorter Zn-O bond length
111 in the former.[18,20,31] Formation of Zn inner-sphere complexes on kaolinite edge sites at
112 high pH and IS results in a larger fractionation than that during the formation of outer-
113 sphere complexes on the basal planes at low pH and IS.[29] Additionally, the distortion
114 of metal octahedron after adsorption makes the metal-O bond less stiff, and can also

115 lead to the enrichment of light isotopes.[10,19] Furthermore, in solution, complexation by
116 inorganic or organic ligands can induce fractionation among various aqueous species,
117 which have different adsorption behaviors on mineral surfaces, and thus affect the
118 overall isotope fractionation.[36] Theoretical calculations showed that successively
119 increasing the number of water molecules of the Cd hydration complexes from 4 to 6
120 favors heavy isotopes. Replacement of the coordinated water molecules around metal
121 by Cl and S gradually makes the complexes lighter but O or N makes the complexes
122 heavier [13,14,37-39] (Table S1).

123 Iron (oxyhydr)oxides are common minerals in soils and sediments and mediate the
124 geochemical behaviors of metal pollutants, especially in tropical and subtropical
125 regions. Despite the fact that Cd is primarily associated with Fe (oxyhydr)oxides in
126 these environments,[9,40] no study so far has investigated Cd isotope fractionation
127 behavior during adsorption and structural incorporation. The objectives of the present
128 study are to determine 1) the direction and magnitude of Cd isotope fractionation during
129 adsorption on different Fe (oxyhydr)oxides (goethite, hematite and ferrihydrite), 2) the
130 effects of pH, IS and initial Cd concentrations on adsorption-induced fractionation, and
131 3) the Cd isotope fractionation during incorporation into goethite.

132 **MATERIALS AND METHODS**

133 **Reagents.** All reagents were used as received and detailed information is provided
134 in the Supporting Information (SI). The Cd isotopic composition of $Cd(NO_3)_2 \cdot 4H_2O$

used for the Cd-doped goethite synthesis is 0.48 ± 0.01‰ relative to NIST SRM 3108 Cd standard (std) according to eq. 1:

$$\delta^{114/110}\mathrm{Cd} = \left[\frac{(^{114}\mathrm{Cd}/^{110}\mathrm{Cd})_{\mathrm{sample}}}{(^{114}\mathrm{Cd}/^{110}\mathrm{Cd})_{\mathrm{std}}} - 1\right] \times 1000 \qquad (1)$$

while the Cd ICP standard used for the adsorption experiments has a $\delta^{114/110}$Cd of -1.71 ± 0.04‰.

Synthesis and Characterization of Iron (Oxyhydr)oxides. Two-line ferrihydrite (2LFh), goethite (Goe) and hematite (Hem) were synthesized according to Cornell and Schwertmann (2003).[41] Ferrihydrite was synthesized by adding 330 mL of 1 M KOH solution to 500 mL of 0.1 M $Fe(NO_3)_3 \cdot 9H_2O$ solution with a drop rate of 1 mL·min^{-1} under stirring until the solution pH reached 7-8, and then the pH was maintained for 1 h by the addition of KOH solution. Goethite was synthesized by adding 180 mL of 5 M KOH solution to 100 mL of 1 M $Fe(NO_3)_3 \cdot 9H_2O$ solution. The obtained suspension was diluted to 2 L with ultrapure water under stirring, and then sealed and aged at 70 °C for 60 h after the pH was adjusted to >13. Hematite was synthesized by slowly adding 60 mL of 1 M $Fe(NO_3)_3 \cdot 9H_2O$ solution to 750 mL boiling ultrapure water at a rate of 0.5 mL·min^{-1} under stirring. After synthesis, the solids were centrifuged, freeze-dried and then stored at 4 °C. The purity of the obtained solids was confirmed by powder X-ray diffraction (XRD) (Fig. S1 and Table S2), while the sample morphologies were measured by electron microscopy (Fig. S2, S3 and Table S3). Goe, Hem and 2LFh have N_2-BET specific surface areas of 37, 56 and 256 m^2·g^{-1} and points of zero charge (PZCs) of ~9.7, ~9.8 and ~8.5, respectively (Fig. S4).

Coprecipitation Experiments. Cd-Fe coprecipitates were obtained by adding $Cd(NO_3)_2$ into $Fe(NO_3)_3$ solution in acid-cleaned 1 L Teflon bottles and adjusting the pH to >13 prior to aging at 70 °C. After aging for 12 and 60 h, 50 mL of the solid and supernatant were collected. The obtained solids were named as 5CdGoe_12h and 5CdGoe_60h. These solids were subsequently treated with 50 mL 0.2 M oxalic acid for 2 h to remove poorly crystalline phases. As-obtained solids were labeled as 5CdGoe_12h_o and 5CdGoe_60h_o. Then these solids were further treated with 50 mL 0.4 M HNO_3 for 0.5 h to remove small goethite particles and/or Cd^{2+} adsorbed on mineral surfaces.[27] The finally obtained solids were named as 5CdGoe_12h_n and 5CdGoe_60h_n. The detailed procedure is depicted in Fig. S5a. Quantitative phase analysis of the solids was conducted using the TOPAS software (DIFFRAC^{plus} TOPAS version 4.2, Bruker-AXS)[27] (Fig. S5c). The obtained solids and supernatants were used for the Cd isotope analysis.

Adsorption Experiments. For adsorption kinetics, 22.2, 44.5 or 89 µM Cd^{2+} was reacted with 1 g·L^{-1} Goe or Hem, or 0.5 g·L^{-1} 2LFh in 0.05 M KNO_3 at pH 7 for 48 h, and aliquot suspensions were collected at predetermined time intervals (Table S4). Adsorption edges were measured over pH 4-8 for 24 h (Table S5). Adsorption isotherms were carried out with initial Cd^{2+} concentrations of 0 - 89.0 µM for Goe or Hem and 0-177.9 µM for 2LFh at pH7 for 24 h (Table S5, S6). Prior to mixing with Cd^{2+} solution, the solids were hydrated in background electrolyte for 24 h. Low (0.05 M) and high (0.36 M) IS were used to determine the IS effects on Cd^{2+} adsorption and

associated isotope fractionation, and NO_3^- was used rather than Cl^- because the former is more common in soil and aquatic systems.

In all experiments, Cd^{2+} was added to the mineral suspensions to obtain a similar surface coverage but prevent Cd precipitation.[42] The suspension pH was maintained via adding 1 M HNO_3 or KOH. At the end of the reactions, the solids and solution were separated through 0.2-μm cellulose membranes. To remove dissolved Cd, the selected Cd-loaded solids (Table S7) were immediately washed sequentially with background electrolyte and ultrapure water, the pH of which were adjusted to that used for adsorption experiments.[20] The cleaned solid (labeled as CdMineral_initial Cd concentration_reaction pH) was collected with membrane filtration, sealed with Kapton tape, and stored at 4 °C within 24 h prior to Cd K-edge extended X-ray absorption fine structure (EXAFS) analysis. For the isotope analysis, experiments of selected pH edge and isotherms (Table S8) were re-conducted in acid-cleaned Teflon vials in the same way as described above.

The Cd concentrations in solutions and solids after digestion were determined using a flame or graphite furnace atomic absorption spectrometer (FAAS or GFAAS, Agilent Technologies 200 Series AA or GTA 120 Graphite Tube Atomizer), depending on Cd concentrations. The detection limit for FAAS is 6.77 $\mu g \cdot L^{-1}$ and the uncertainty is 0.3% while those for GFAAS are 0.06 $\mu g \cdot L^{-1}$ and 2.7% respectively. Control experiments with no Cd^{2+} addition to Goe suspension gave a Cd concentration of 7.35 ± 0.07 $\mu g \cdot L^{-1}$ by FAAS. As the latter value was substantial, it was subtracted from sample Cd concentrations. Duplicate or triplicate experiments were carried out to

198 ensure reproducibility.

199 **Cadmium Isotopes Analysis.** Sample solutions were evaporated and the solids of
200 the coprecipitation and adsorption experiments (with membrane) were digested prior to
201 isotope analysis.

202 About 600 ng Cd of each sample was weighed and placed into Teflon beakers, and
203 then mixed with 0.6 mL of 1 mg·L^{-1} ^{111}Cd-^{110}Cd double spike solution to achieve a Cd
204 spike–sample ratio of ~1. Detailed information on the double spike solution, sample
205 digestion and Cd chemical purification was reported in our previous studies,[43,44] and
206 the Cd recovery rate was > 95% for all samples.

207 Cadmium isotopic ratios were measured using a Thermo Scientific Neptune plus
208 MC-ICP-MS with a Ni 'Standard' sampler and Ni 'x-type' skimmer cones at the State
209 Key Laboratory of Ore Deposit Geochemistry, Institute of Geochemistry, CAS. A
210 nebulizer–spray chamber (with an uptake rate of ~50 μL·min^{-1}) was used as sample
211 introduction system and the low-resolution entrance slit was chosen throughout the
212 analysis. The instrumental baseline and peak center were done before each sample
213 (standard) analysis. Each measurement included 60 integrations of 4.194 s in 2 blocks
214 of 30 cycles, and we also measured ^{105}Pd at every start of 10 cycles with integrations of
215 2.097 s, followed by a 120 s washing with 5 % HNO_3 to lower the Cd signal to the
216 original background level (< 0.1 mV). The instrumental sensitivity was about 28 V/ppm.
217 In this study, the double spike method was employed to correct the mass bias. All
218 samples and bracketing reference solutions were diluted to 400 ng·mL^{-1} (sample (200
219 ng·mL^{-1}) + double spike (200 ng·mL^{-1})) within a 10 % difference.[45]

Using a MATLAB-based script and the measured double-spike data, Cd isotope compositions of samples and standards were calculated.[43] The NIST SRM 3108 Cd (lot no. 130116) was used as a zero reference standard. The JMC (lot no.74-075219k) and Nancy Spex Cd solution (CRPG, France), as well as a solid Cd isotope reference (NOD-P-1, manganese-nodule), were additionally used as secondary reference standards. The measured values for JMC Cd ($\delta^{114/110}$Cd = -1.68 ± 0.08 ‰; 2SD, n=4), Nancy Spex Cd ($\delta^{114/110}$Cd = -0.11 ± 0.06 ‰; 2SD, n=4) and NOD-P-1 ($\delta^{114/110}$Cd = 0.13 ± 0.08 ‰; 2SD, n=2) agreed well with previous results.[43,46] The long-term reproducibility of this method was better than ±0.08‰ (2SD; N=20) with $\delta^{114/110}Cd_{Nancy\text{-}Spex}$ values ranging from -0.08 to -0.15‰. The isotopic fractionation of Cd ($\Delta^{114/110}Cd_{solid\text{-}solution}$) between adsorbed phase and aqueous phase is defined as eq. 2:

$$\Delta^{114/110}Cd_{solid\text{-}solution} = \delta^{114/110}Cd_{solid} - \delta^{114/110}Cd_{solution} \quad (2)$$

EXAFS Data Collection and Analysis. The Cd K-edge EXAFS spectra were collected on beamline BL14W1 at Shanghai Synchrotron Radiation Facility (SSRF) at room temperature.[27] Cadmium-containing samples (0.9-4.4 wt.% Cd) and 50 mM $Cd(NO_3)_2$ solution were measured with a Si (311) double-crystal monochromator in fluorescence mode while β-$Cd(OH)_2$ in transmission mode. A silver metal foil was used for energy calibration (25529 eV). The data processing was performed using the IFEFFIT software.[47] The parameters for background removal were: E_0=26714 eV, *k*-weight=2 and R_{bkg}=1.0. Structural parameters (R, CN, and σ^2) were obtained by fitting the experimental k^3-weighted spectra to the standard equation.[48] FEFF7 was used to calculate the phase and amplitude functions for single-scattering paths,[49] based on

structure models of Cd-doped goethite (ICSD 71810) and ferrihydrite (ICSD 158475). An amplitude reduction factor (S_0^2) of 0.95 was adopted from a previous study.[50] During the EXAFS analysis, the first Cd-O shell fitting was conducted assuming a Gaussian or a non-Gaussian distribution model, with a third cumulant in the latter to account for the asymmetry of [CdO_6] octahedron.[51,52] More details are provided in the SI.

RESULTS

Macroscopic Cd^{2+} Adsorption Behavior. Iron (oxyhydr)oxides have high adsorption reactivity towards Cd^{2+}. The adsorption edges, kinetics and isotherms show similar patterns for the three mineral phases (Fig. 1). Adsorption occurs rapidly initially and then increases slowly during the first 12 h. After 24 h, pseudo equilibria were reached and the Cd adsorption densities remain almost constant. After 48 h, the Cd^{2+} adsorption density on 2LFh is 1.7-2 times that on Hem or Goe (Fig. 1a), owing to the higher initial Cd^{2+} concentration and lower mineral concentration (Table S4). With increasing pH, Cd^{2+} adsorption increases slightly below pH6.0 but dramatically over pH6.0−8.0 (Fig. 1b, Table S5), characteristic of Cd^{2+} adsorption on Fe (oxyhydr)oxides.[53-55] Further, Cd^{2+} adsorption increases with increasing initial Cd^{2+} concentration (Fig. 1c-e). The maximum Cd^{2+} adsorption densities obtained by Langmuir isotherm fitting, are 1.12 and 1.23 μmol·m^{-2} for Goe, 0.89 and 0.57 μmol·m^{-2} for Hem, and 1.21 and 1.10 μmol·m^{-2} for 2LFh at low and high IS, respectively (Table S6).

Cadmium Binding Environments in Adsorbed and Coprecipitated Samples. The k^3-weighted Cd K-edge EXAFS spectra and the corresponding Fourier transforms (FTs) of Cd-loaded 2LFh samples are distinct from those of $Cd(NO_3)_2$ solution and β-$Cd(OH)_2$ (Fig. S6), indicating the formation of inner-sphere complexes on 2LFh surfaces without precipitation of Cd hydroxide. For the adsorption samples, including a third cumulant in the first shell of the EXAFS fitting (Fig. S6 and Table 1) improves the fitting quality by reducing χ^2 and R-factor by 5-42% compared to that without a third cumulant (Fig. S7 and Table S6). Thus, a third cumulant is included for spectral fitting of all samples and standards. The EXAFS fitting demonstrates an average Cd-O distance of 2.29 ± 0.02 Å in $Cd(NO_3)_2$ solution, consistent with previously reported values.[24,56,57] β-$Cd(OH)_2$ has a Cd-O bond length of 2.31 ± 0.02 Å in the [CdO_6] unit and an edge-sharing Cd-Cd distance of 3.51 ± 0.01 Å, which also agree with literatures.[25,27] For the Cd-adsorbed 2LFh samples, the Cd-O distances are 2.28-2.32 Å. Only one Cd-Fe shell with distances ranging from 3.31-3.36 Å is needed to fit the R+ΔR ~ 2.9 Å peak, suggesting Cd^{2+} mainly exists as bidentate edge-sharing complexes.[24] Moreover, these distances are almost constant independent of pH or surface loading, suggesting the formation of the same type of surface complexes.

TEM and powder XRD analyses show that the Cd-Fe coprecipitates aging at 70 °C for 12 and 60 h are mixtures of ferrihydrite and goethite. A XRD quantitative phase analysis shows that 5CdGoe_12h and 5CdGoe_60h contain 76.1 ± 2.3% and 7.1 ± 2.5% ferrihydrite, respectively (Fig. S5c). The oxalate removes all ferrihydrite and subsequent HNO_3 treatment removes Cd^{2+} adsorbed on goethite surfaces, yielding pure

Cd-doped goethite (Fig. S5b,c). The oxalate treatment removes 84.9 ± 0.8% Cd and 84.3 ± 0.4% Fe from 5CdGoe_12h, and 27.9 ± 0.2% Cd and 14.1 ± 0.1% Fe from 5CdGoe_60h (Fig. S5a). These contents of Fe dissolved are consistent with the ferrihydrite proportions determined by XRD analysis. The HNO_3 treatment removes 12.7 ± 0.1% Cd and 12.8 ± 0.0% Fe from Fe5CdGoe_12h_o, and 2.2 ± 0.0% Cd and 1.0 ± 0.0% Fe from 5CdGoe_60h_o (Fig. S5a). All the solids obtained have Cd/Fe molar ratios of ~0.05. The lattice parameters of Cd-doped goethites determined by Rietveld structure refinement[58] are expanded compared to those of Goe (Table S2), suggesting the incorporation of Cd into the goethite lattice[27,59]. This is further confirmed by EXAFS analysis. The EXAFS oscillation of 5CdGoe_60h_n has a special feature at ~ 6.4 $Å^{-1}$ (array in Fig. S6A), characteristic of Cd-doped goethite.[25,57] The EXAFS fitting indicates a Cd-O distance of 2.29 ± 0.06 Å and a Cd-Fe distance of 3.07 ± 0.04 Å. The later distance corresponds to the Cd-Fe pairs between edge-sharing [CdO_6] and [FeO_6] units along the c axis in the Cd-doped goethite structure.[25,60]

Isotopic Behavior of Cd^{2+} during Adsorption on Fe (oxyhydr)oxides. The isotopic compositions ($\delta^{114/110}Cd$) of dissolved and adsorbed Cd^{2+} during isotherm adsorption indicate light Cd isotopes are preferentially adsorbed on the solids (Fig. 2, Fig. S8a-c and Table S8). The isotope fractionations ($\Delta^{114/110}Cd_{solid\text{-}solution}$) vary from -0.63 ± 0.02‰ to -0.47 ± 0.03‰ for Goe, and from -0.45 ± 0.05‰ to -0.35 ± 0.06‰ for 2LFh at low IS. While IS affects the Cd^{2+} adsorption density on Hem (Fig. 1), the isotope fractionations at low (-0.55 ± 0.11‰, n=7) and high IS (-0.52 ± 0.06‰, n=3)

are statistically the same. pH does not affect the fractionation magnitude, either (Fig. 2, Fig. S8d-f, S9).

The $\delta^{114/110}Cd$ values represented as a function of Cd adsorbed fractions (f) are used to identify whether isotopic equilibrium is attained between adsorbed and aqueous Cd^{2+} (Fig. 2). Both the equilibrium model, where adsorbed Cd isotopically exchanges with aqueous Cd in a closed system (eq. 3), and the Rayleigh model, where the adsorbed Cd is isolated from isotopic exchange (eq. 4), were used to fit the data:

$$\delta^{114/110}Cd_{solution} = \frac{\delta^{114/110}Cd_{stock} - 1000 \cdot f \cdot (\alpha_{solid\text{-}solution} - 1)}{1 - f + (f \cdot \alpha_{solid\text{-}solution})} \quad \text{(equilibrium model)} \quad (3)$$

$$\delta^{114/110}Cd_{solution} = (1000 + \delta^{114/110}Cd_{stock}) \cdot (1 - f)^{(\alpha_{solid\text{-}solution} - 1)} - 1000 \quad \text{(Rayleigh model)} \quad (4)$$

where $\alpha_{solid\text{-}solution}$ denotes the isotope fractionation factor between dissolved and adsorbed Cd, and $\delta^{114/110}Cd_{stock}$ is the measured value for stock solution.

The equilibrium model fits the data much better than the Rayleigh model, confirming an equilibrium isotopic exchange process (Fig. 2). The fractionation factors, obtained by averaging the two values determined from $\delta^{114/110}Cd$ in solution and in solid separately using the equilibrium model, are 0.99949 ± 0.00004, 0.99946 ± 0.00010 and 0.99945 ± 0.00003 for Goe, Hem and 2LFh, respectively. According to $\alpha_{solid\text{-}solution}$, the isotopic fractionation between adsorbed and dissolved Cd can be calculated by eq. 5:

$$\Delta^{114/110}Cd_{solid\text{-}solution} \cong 1000 \times \ln\alpha_{solid-solution} \quad (5)$$

The theoretical $\Delta^{114/110}Cd_{solid\text{-}solution}$ values are -0.51 ± 0.04‰, -0.54 ± 0.10‰ and -0.55 ± 0.03‰ for Goe, Hem and 2LFh, respectively.

Isotopic Behavior During Cd^{2+} Coprecipitation with Goethite. The isotope composition analysis (Fig. 3) demonstrates that $\delta^{114/110}Cd_{soild\text{-}solution}$ of 5CdGoe_12h and

the solution are 0.44 ± 0.07‰ and 0.64 ± 0.08‰, respectively. After aging for additional 48 h, the $\delta^{114/110}$Cd for 5CdGoe_60h becomes 0.50 ± 0.03‰ while that in the solution substantially decreases to 0.24 ± 0.01‰. After the oxalate treatment of 5CdGoe_60h, $\delta^{114/110}$Cd in the solution (oxalate) decreases to 0.08 ± 0.00‰ while that in the solid (5CdGoe_60h_o) increases to 0.65 ± 0.03‰. The subsequent HNO_3 treatment of 5CdGoe_60h_o results in a slight increase of $\delta^{114/110}$Cd in the solution (HNO_3) and an almost unchanged $\delta^{114/110}$Cd (0.62 ± 0.04‰) in the obtained 5CdGoe_60h_n.

Further, the isotope fractionation magnitude during Cd incorporation into goethite lattice was calculated. Since all Cd is transferred to the solid (Fig. 3a and Fig. S5a), the isotope signals recorded during this process are listed in eqs. 6-7:

$$\delta^{114/110}Cd_{stock\ solution} = f_1\times\delta^{114/110}Cd_{adsorbed\_ferrihydrite} + f_2\times\delta^{114/110}Cd_{HNO3} + f_3\times\delta^{114/110}Cd_{5CdGoe\_60h\_n} \quad (6)$$

$$\Delta^{114/110}Cd_{stock\ solution} = 0 = f_1\times\Delta^{114/110}Cd_{adsorbed\_ferrihydrite} + f_2\times\Delta^{114/110}Cd_{HNO3} + f_3\times\Delta^{114/110}Cd_{5CdGoe\_60h\_n} \quad (7)$$

Where f_1, f_2 and f_3 are the fractions of Cd adsorbed on the ferrihydrite phase that was removed by the oxalate treatment of 5CdGoe_60h, adsorbed on the goethite surfaces that was removed by the HNO_3 treatment of 5CdGoe_60h_o and that incorporated into the 5CdGoe_60h_n mineral lattice, respectively. However, based on the mass balance for 5CdGoe_60h, f_2 (1.59 ± 0.01%) is negligible. The $\delta^{114/110}Cd_{adsorbed\_ferrihydrite}$ is 0.08 ± 0.00‰, and the adsorption-induced Cd fractionation on 2LFh (-0.55 ± 0.03‰) determined in the adsorption experiments can be used for $\Delta^{114/110}Cd_{adsorbed\_ferrihydrite}$. Based on eqs. 6-7, the $\delta^{114/110}Cd_{5CdGoe\_60h\_n}$ and $\Delta^{114/110}Cd_{5CdGoe\_60h\_n}$ are calculated to be 0.65 ± 0.01‰ and 0.22 ± 0.01‰, of which the former agrees well with the measured

343 value for 5CdGoe_60h_n (Fig. 3a and Fig. S5a). All these results clearly confirm that,
344 incorporation of Cd into goethite lattice substantially enriches heavy Cd isotopes.

345 **DISCUSSION**

346 **Cadmium Isotope Fractionation During Adsorption onto Iron**
347 **(Oxyhydr)oxides.** Heavy isotopes are generally enriched in substances with stronger
348 bonds and shorter bond lengths[10,35], such as the enrichment of heavy Zn and Cu isotopes
349 on solids during adsorption on Fe and Al oxides[20,61]. In contrast, the present study
350 shows the preferential adsorption of light Cd^{2+} isotopes onto Fe (oxyhydr)oxides. A
351 similar phenomenon was observed for Ni^{2+} adsorption on Fe oxides,[19] in which
352 distortion of adsorbed [NiO_6] was proposed to account for the apparent anomaly. [CdO_6]
353 distortion during adsorption on manganite was also previously proposed based on
354 EXAFS analysis.[52] The present Cd K-edge EXAFS fittings with the third cumulant
355 greatly improve the fit quality compared to that without the third cumulant, and both
356 demonstrate almost the same structural parameters for $Cd(NO_3)_2$ or β-$Cd(OH)_2$,
357 confirming the regular [CdO_6] structure.[52] However, the first Cd-O shell distances in
358 the Cd adsorbed samples derived from fitting with a third cumulant (2.28-2.32 Å) are
359 substantially longer than those obtained without a third cumulant (2.24-2.26 Å).
360 Additionally, the third cumulants, which are measures of disorder,[52] for Cd-sorbed
361 samples (0.0007-0.0011) are larger than those for $Cd(NO_3)_2$ and β-$Cd(OH)_2$ (0.0003-
362 0.0004). We thus conclude that [CdO_6] adsorbed on these Fe (oxyhydr)oxide surfaces

363 is highly distorted (Table 1), which probably accounts for the enrichment of light Cd
364 isotope on the solids.

365 The fractionation magnitude of Zn or Ni during adsorption on Fe (oxyhydr)oxides
366 depends on the mineral phases involved.[20,21] In contrast, our results show that Cd
367 adsorptions on Goe, Hem and 2LFh result in the same fractionation magnitudes. The
368 differences in isotope fractionations for Cd compared to Zn and Ni during adsorption
369 on Fe (oxyhydr)oxides can be understood by considering their different metal
370 adsorption mechanisms. For example, the tetrahedral coordination of adsorbed Zn on
371 ferrihydrite results in a larger Zn fractionation than during the octahedral coordination
372 of adsorbed Zn on goethite[20], whereas a stronger Ni complexation on ferrihydrite than
373 on goethite results in smaller Ni fractionation by ferrihydrite than by goethite.[21]
374 However, in comparison with the first-row transition metals, Cd^{2+} may be more prone
375 to form outer-sphere complexes.[15, 62, 63] Ionic strength affects Cd adsorption on the three
376 Fe (oxyhydr)oxides with a stronger effect on Hem than on Goe and 2LFh, suggesting
377 the possible formation of outer-sphere complexes on Hem. The Cd inner-sphere
378 complexes formed on Hem are probably also different from those on Goe and 2LFh.
379 Indeed, the geometry of adsorbed Cd on 2LFh, as measured in the present study, is
380 similar to those of adsorbed Cd on goethite reported previously.[24,25,64-66] No EXAFS
381 information for Cd adsorption on hematite is available yet. However, crystallographic
382 studies demonstrate that, goethite needles and hematite cubic particles expose different
383 facets, which have different surface charge properties, and thus possess different cation
384 adsorption characteristics.[67-69] Though both outer- and inner-spherical complexation of

Cd can induce isotope fractionations,[15,29] the observed same Cd isotope fractionation magnitudes on these Fe (oxyhydr)oxides clearly suggest that the types of Cd binding complexes do not impact the final isotope fractionations.

Further, though high IS suppresses Cd adsorption on Hem, the Cd isotope fractionation magnitudes on Hem at high and low IS conditions are almost the same, which is different from that during Zn and Cd adsorption onto Mn oxides.[10,31] Calculations of aqueous Cd speciation at low and high KNO_3 concentrations using Visual MINTEQ 3.1[70] indicate Cd occurs dominantly as $Cd(H_2O)_6^{2+}$ (86%) with 13% $Cd(NO_3)(H_2O)_5^{+}$ at low IS, and $Cd(H_2O)_6^{2+}$ and $Cd(NO_3)(H_2O)_5^{+}$ are almost equal (48% vs. 45%) at high IS. However, the reduced partition function ratios $10^3\ln(\beta_{114-110})$ for $Cd(NO_3)(H_2O)_5^{+}$ and $Cd(H_2O)_6^{2+}$ are almost similar (2.323 ± 0.034 vs. 2.299 ± 0.028) (Table S1),[13] thus the increase in the proportion of the former with increasing IS has almost no effect on Cd isotope fractionation magnitude during adsorption on Hem. This suggests that the changes in aqueous speciation also have no effect on the final Cd isotope fractionation. Conclusively, during Cd^{2+} adsorption onto these Fe (oxyhydr)oxides, the fractionation magnitudes and the fractionation mechanism ($[CdO_6]$ distortion) are independent of the types of Cd binding sites on minerals and environmental conditions.

Cadmium Isotope Fractionation During Coprecipitation with Goethite. Almost all Cd is retained in 5CdGoe_12h and 5CdGoe_60h, thus the $\delta^{114/110}Cd$ of these solids are equal to the Cd stock solution (0.48 ± 0.01‰) (Fig. 3 and Fig. S5a). Oxalate treatment of 5CdGoe_60h removes all the Cd associated with ferrihydrite. This leads

to the decrease of the $\delta^{114/110}$Cd value in the resulting solution, which is consistent with the expected fractionation as this part of Cd is probably adsorbed on ferrihydrite[27] and thus has a large negative fractionation according to the results of adsorption-induced Cd isotope fractionation on ferrihydrite (Fig. 2). Further treating 5CdGoe_60h_o with HNO_3 removes Cd adsorbed on goethite particles.[27] The extracted solution is enriched in light isotopes compared to 5CdGoe_60h_o. This is also consistent with the expected fractionation as the Cd adsorbed on goethite is enriched in light isotopes (Fig. 2).

Several studies have reported isotope fractionation induced by metal incorporation into mineral structures. This may predominantly involve two mechanisms: preferential retention of one species in the mineral after isotopic exchange equilibrium among various aqueous species, and direct preferential enrichment of one aqueous isotope owing to, for example, coordination chemistry differences or kinetic effects. Light Cd isotopes are enriched in the solid during CdS precipitation, which is controlled by the isotope equilibrium between aqueous Cd species.[12] During Cd incorporation into calcite in artificial seawater, light isotopes are preferred in the solid following a kinetic isotope effect, ascribing to the retardation of crystal growth and Cd uptake caused by overwhelming occupancy of the active surface sites by the major ions (particularly Na^+ and K^+).[11] Recently, aqueous Zn^{2+} was reported to firstly adsorb onto calcite growth sites by forming tetrahedral inner-sphere complexes enriching heavy isotopes and then incorporate into the crystal lattice by increasing the coordination number to 6 without further isotope fractionation[34].

We obtain a $\Delta^{114/110}Cd_{solid\text{-}solution}$ of ~0.22‰ for incorporation of Cd into the goethite structure. Goethite formation from ferrihydrite likely involves formation of reactive and labile small ferrihydrite particles and subsequent dissolution to provide dissolved Fe^{3+} for goethite crystallization in bulk solution,[41,71-73] which can be divided into two stages (Fig. 3b):

In stage 1 (0-t2 in Fig. 3b), coprecipitation of Cd with Fe at a high OH^- concentration probably sequesters all the Cd and Fe into ferrihydrite at time t2.[73] The $\delta^{114/110}Cd$ of the "absolutely pure" ferrihydrite should be ~0.48‰, while that in the corresponding equilibrium solution should be larger than 0.64‰. The enrichment of heavy isotopes in this solution probably results from a kinetic isotope effect in that the presence of 0.45 M K^+ in the initial reactant blocks the active sites on the primary Fe (oxyhydr)oxide nanoparticles, and lighter isotopes are adsorbed faster by the solid.[11,73] However, this kinetic effect is progressively removed within few hours (t1 in Fig. 3b).[10] Further, the formed ferrihydrite particles greatly adsorb light Cd isotopes through the whole stage 1 (0-t2 in Fig. 3b), and thus leave heavy isotopes in solutions, according to the results of Cd isotope fractionation during adsorption experiments (Fig. 2).

Subsequently, stage 2 (t2-60 h in Fig. 3b) starts. Ferrihydrite particles slowly dissolve, releasing soluble Fe and Cd species into the solution. The Cd released is expected to be relatively heavy isotopically, based on the fact that many weathering processes of Cd-containing minerals preferentially release heavy isotopes into the fluids[4,17,46] and that the remaining ferrihydrite retains light isotopes. As the dissolved Fe units ($[Fe(OH)_4]^-$)[41,73] nucleate and grow to less soluble goethite, monovalent Cd

450 species ($[Cd(OH)_3]^-$) in solution, which are the most suitable growth units[41] and enrich
451 heavy isotopes[13], interact with the goethite growth sites via ion-by-ion attachment[34].
452 This leads to the enrichment of heavy Cd isotopes in the goethite structures. The slow
453 dissolution of ferrihydrite results in the coexistence of goethite and ferrihydrite
454 particles in this stage. This is confirmed by the powder XRD quantitative phase
455 analysis and TEM of 5CdGoe_12h and 5CdGoe_60h (Fig. S5b,c). The part of Cd
456 associated with ferrihydrite particles in these solids is probably enriched in light
457 isotopes, as evidenced by the isotope composition of the resulting solution after
458 treatment of 5CdGoe_60h with oxalate (Fig. 3a). In contrast, the goethite particles in
459 the solids during this stage retain heavy Cd isotopes. This is convincingly supported
460 by the isotope composition analysis of 5CdGoe_60h_o and 5CdGoe_60h_n (Fig. 3a),
461 which are pure Cd-doped goethites (Fig. S5b,c).

462 In conclusion, enrichment of heavy Cd isotopes in Cd-doped goethite crystals is
463 achieved probably during the ferrihydrite dissolution-goethite crystallization processes.
464 Though the enrichment of heavy isotopes by incorporation into the Mn oxide structure
465 is also observed for Ni, the fractionation magnitude is not given.[22] All these results
466 suggest that the incorporation of octahedrally coordinated cations into Fe/Mn
467 (oxyhydr)oxides enriches heavier isotopes relative to solutions. Nonetheless, the metal
468 isotope fractionation behaviors and mechanisms in these processes are worthy of
469 further study.

470 **ENVIRONMENTAL IMPLICATIONS**

Cadmium isotope composition reflects Cd geochemical cycling and helps track Cd anthropogenic sources.[3,16,74,75] However, based on previous research with other metals, interactions with minerals are likely to affect Cd isotope compositions in environmental systems. To the best of our knowledge, the present study is the first to investigate Cd isotope fractionation during adsorption on and isomorphous substitution in Fe (oxyhydr)oxides. Preferential adsorption of light Cd isotopes onto Fe (oxyhydr)oxides, as well as on Mn oxides[10] and humic acids[15], explains the enrichment of light isotopes in soils and sediments relative to the fluids.[3,4,9,46,76] Considering the high abundance of Fe (oxyhydr)oxides in tropical and subtropical soils,[9,40] they probably play an important role in controlling Cd isotope characteristics as other soil components, e.g., clays, Mn oxides and organic matters. Our results suggest that the enrichment of lighter Cd isotopes in Fe-Mn nodules in the lower layers of soil profiles compared to the surrounding soils observed previously[9] is likely to be caused by enrichment of light Cd isotopes on goethite surfaces in the nodules. Our study also suggests that Fe (oxyhydr)oxide transformation between different phases can also result in Cd isotope fractionation. These geochemical processes greatly complicate the potential use of Cd isotopes to identify Cd sources.[9,77] Our results are consistent with the recently proposed ferrihydrite dissolution-goethite crystallization mechanism, and suggest that metal isotope fractionation behavior by adsorption or coprecipitation with minerals provides insights into mineral transformation pathways and mechanisms that are hard to elucidate with other techniques[73]. Future studies are warranted, including

coprecipitation of different heavy metals with Fe minerals and investigations into the effects of prolonged aging, ligands and temperature.

ASSOCIATED CONTENT

Supporting Information

The Supporting Information is available free of charge at http://pubs.acs.org, including reagent information, a summary of bond length, coordination number and reduced partition function ratio for typical metals (Cd^{2+}, Zn^{2+} and Ni^{2+}) complexed by H_2O (free hydrated ion), and typical inorganic ligands (Cl^-, NO_3^-, HS^- and OH^-); powder XRD, chemical composition, zeta potential, TEM and SEM analysis of obtained minerals; illustration of experimental schedules for isotope fractionation analysis during Cd^{2+} coprecipitation with goethite; Cd^{2+} macroscopic adsorption data for kinetic, adsorption edge and isotherms; Details on Cd K-edge EXAFS data collection and analysis, and the EXAFS fitting results; Cd isotope compositions in solid and aqueous phases, mass balance and fractionation.

AUTHOR INFORMATION

Corresponding Authors

*Phone: +(86 27) 87280271. E-mail: yinhui666@mail.hzau.edu.cn; zhuchuanwei@mail.gyig.ac.cn

ORCID

Hui Yin: 0000-0003-3060-7025

Wei Li: 0000-0002-0789-0320

Mengqiang Zhu: 0000-0003-1739-1055

Caroline L. Peacock: 0000-0003-3754-9294

Notes

The authors declare no competing financial interest.

ACKNOWLEDGMENTS

The authors greatly thank the Associate Editor Prof. Dr. T. David Waite and Dr. Damien Guinoiseau and other three anonymously reviewers for their thoughtful comments and suggestions. Prof. Susan H. Little at University College London, Dr. Wenxian Gou at Nanjing University and Ms. Lena Chen at University of Leeds are gratefully thanked for helpful comments and discussions. Prof. Alain Manceau at ISTerre, Université Grenoble Alpes-CNRS is also gratefully thanked for helpful discussions on Cd^{2+} adsorption on goethite. The authors gratefully thank the Natural Science Foundations of China (Nos. 41771267, 42077015), the National Key Research and Development Program of China (No. 2016YFD0800403), Key Science and Technology Projects of Inner Mongolia autonomous region (No. 2019ZD001), and the Fundamental Research Funds for the Central Universities (Grant 103-510320036) for financial support. This work was financially supported by Royal Society Newton Mobility Grant (IEC/NSFC/191423). Caroline L. Peacock gratefully acknowledges Royal Society Wolfson Research Merit Award (WRM/FT/170005).

REFERENCES

(1) Janssen, D. J.; Abouchami, W.; Galer, S. J. G.; Purdon, K. B.; Cullen, J. T. Particulate cadmium stable isotopes in the subarctic northeast Pacific reveal dynamic Cd cycling and a new isotopically light Cd sink. *Earth Planet. Sci. Lett.* **2019,** *515*, 67-78.

(2) Godt, J.; Scheidig, F.; Grosse-Siestrup, C.; Esche, V.; Brandenburg, P.; Reich, A.; Groneberg, D. A. The toxicity of cadmium and resulting hazards for human health. *J. Occup. Med. Toxicol.* **2006,** *1*.

(3) Zhou, J.-W.; Li, Z.; Liu, M.-S.; Yu, H.-M.; Wu, L.-H.; Huang, F.; Luo, Y.-M.; Christie, P. Cadmium isotopic fractionation in the soil–plant system during repeated phytoextraction with a cadmium hyperaccumulating plant species. *Environ. Sci. Technol.* **2020,** *54*, (21), 13598-13609.

(4) Imseng, M.; Wiggenhauser, M.; Keller, A.; Müller, M.; Rehkämper, M.; Murphy, K.; Kreissig, K.; Frossard, E.; Wilcke, W.; Bigalke, M. Fate of Cd in agricultural soils: A stable isotope approach to anthropogenic impact, soil formation, and soil-plant cycling. *Environ. Sci. Technol.* **2018,** *52*, (4), 1919-1928.

(5) Chrastný, V.; Čadková, E.; Vaněk, A.; Teper, L.; Cabala, J.; Komárek, M. Cadmium isotope fractionation within the soil profile complicates source identification in relation to Pb–Zn mining and smelting processes. *Chem. Geol.* **2015,** *405*, 1-9.

(6) Yang, W.-J.; Ding, K.-B.; Zhang, P.; Qiu, H.; Cloquet, C.; Wen, H.-J.; Morel, J.-L.; Qiu, R.-L.; Tang, Y.-T. Cadmium stable isotope variation in a mountain area impacted by acid mine drainage. *Sci. Total Environ.* **2019,** *646*, 696-703.

(7) Salmanzadeh, M.; Hartland, A.; Stirling, C. H.; Balks, M. R.; Schipper, L. A.; Joshi, C.; George, E. Isotope tracing of long-term cadmium fluxes in an agricultural soil. *Environ. Sci. Technol.* **2017,** *51*, (13), 7369-7377.

(8) Barraza, F.; Moore, R. E. T.; Rehkämper, M.; Schreck, E.; Lefeuvre, G.; Kreissig, K.; Coles, B. J.; Maurice, L. Cadmium isotope fractionation in the soil–cacao systems of Ecuador: a pilot field study. *RSC Adv.* **2019,** *9*, (58), 34011-34022.

(9) Gao, T.; Liu, Y.; Xia, Y.; Zhu, J.-M.; Wang, Z.; Qi, M.; Liu, Y.; Ning, Z.; Wu, Q.; Xu, W.; Liu, C. Cadmium isotope compositions of Fe-Mn nodules and surrounding soils: Implications for tracing Cd sources. *Fund. Res.* **2021**.

(10) Wasylenki, L. E.; Swihart, J. W.; Romaniello, S. J. Cadmium isotope fractionation during adsorption to Mn oxyhydroxide at low and high ionic strength. *Geochim. Cosmochim. Acta* **2014,** *140*, 212-226.

(11) Horner, T. J.; Rickaby, R. E. M.; Henderson, G. M. Isotopic fractionation of cadmium into calcite. *Earth Planet. Sci. Lett.* **2011,** *312*, (1), 243-253.

(12) Guinoiseau, D.; Galer, S. J. G.; Abouchami, W. Effect of cadmium sulphide precipitation on the partitioning of Cd isotopes: Implications for the oceanic Cd cycle. *Earth Planet. Sci. Lett.* **2018,** *498*, 300-308.

(13) Yang, J.; Li, Y.; Liu, S.; Tian, H.; Chen, C.; Liu, J.; Shi, Y. Theoretical calculations of Cd isotope fractionation in hydrothermal fluids. *Chem. Geol.* **2015,** *391*, 74-82.

(14) Zhao, Y.; Li, Y.; Wiggenhauser, M.; Yang, J.; Sarret, G.; Cheng, Q.; Liu, J.; Shi, Y. Theoretical isotope fractionation of cadmium during complexation with organic ligands. *Chem. Geol.* **2021,** *571*, 120178.
(15) Ratié, G.; Chrastný, V.; Guinoiseau, D.; Marsac, R.; Vaňková, Z.; Komárek, M. Cadmium isotope fractionation during complexation with humic acid. *Environ. Sci. Technol.* **2021**.
(16) Wiggenhauser, M.; Aucour, A.-M.; Bureau, S.; Campillo, S.; Telouk, P.; Romani, M.; Ma, J. F.; Landrot, G.; Sarret, G. Cadmium transfer in contaminated soil-rice systems: Insights from solid-state speciation analysis and stable isotope fractionation. *Environ. Pollut.* **2021,** *269*, 115934.
(17) Zhu, C.; Wen, H.; Zhang, Y.; Yin, R.; Cloquet, C. Cd isotope fractionation during sulfide mineral weathering in the Fule Zn-Pb-Cd deposit, Yunnan Province, Southwest China. *Sci. Total Environ.* **2018,** *616-617*, 64-72.
(18) Gou, W.; Li, W.; Ji, J.; Li, W. Zinc isotope fractionation during sorption onto Al oxides: Atomic level understanding from EXAFS. *Environ. Sci. Technol.* **2018,** *52*, (16), 9087-9096.
(19) Wasylenki, L. E.; Howe, H. D.; Spivak-Birndorf, L. J.; Bish, D. L. Ni isotope fractionation during sorption to ferrihydrite: Implications for Ni in banded iron formations. *Chem. Geol.* **2015,** *400*, 56-64.
(20) Juillot, F.; Maréchal, C.; Ponthieu, M.; Cacaly, S.; Morin, G.; Benedetti, M.; Hazemann, J. L.; Proux, O.; Guyot, F. Zn isotopic fractionation caused by sorption on goethite and 2-Lines ferrihydrite. *Geochim. Cosmochim. Acta* **2008,** *72*, (19), 4886-4900.
(21) Gueguen, B.; Sorensen, J. V.; Lalonde, S. V.; Peña, J.; Toner, B. M.; Rouxel, O. Variable Ni isotope fractionation between Fe-oxyhydroxides and implications for the use of Ni isotopes as geochemical tracers. *Chem. Geol.* **2018,** *481*, 38-52.
(22) Sorensen, J. V.; Gueguen, B.; Stewart, B. D.; Peña, J.; Rouxel, O.; Toner, B. M. Large nickel isotope fractionation caused by surface complexation reactions with hexagonal birnessite. *Chem. Geol.* **2020,** *537*, 119481.
(23) Yuan, Q.; Li, P.; Liu, J.; Lin, Y.; Cai, Y.; Ye, Y.; Liang, C. Facet-dependent selective adsorption of Mn-doped α-Fe_2O_3 nanocrystals toward heavy-metal ions. *Chem. Mater.* **2017,** *29*, (23), 10198-10205.
(24) Tiberg, C.; Gustafsson, J. P. Phosphate effects on cadmium(II) sorption to ferrihydrite. *J. Colloid Interface Sci.* **2016,** *471*, 103-111.
(25) Spadini, L.; Manceau, A.; Schindler, P. W.; Charlet, L. Structure and stability of Cd^{2+} surface complexes on ferric oxides: 1. Results from EXAFS spectroscopy. *J. Colloid Interface Sci.* **1994,** *168*, (1), 73-86.
(26) Singh, B.; Gräfe, M.; Kaur, N.; Liese, A. Chapter 8 - Applications of Synchrotron-Based X-Ray Diffraction and X-Ray Absorption Spectroscopy to the Understanding of Poorly Crystalline and Metal-Substituted Iron Oxides. In *Developments in Soil Science*, Balwant, S.; Markus, G., Eds. Elsevier: 2010; Vol. 34, pp 199-254.
(27) Liu, L.; Wang, X.; Zhu, M.; Ma, J.; Zhang, J.; Tan, W.; Feng, X.; Yin, H.; Liu, F. The speciation of Cd in Cd–Fe coprecipitates: Does Cd substitute for Fe in goethite

structure? *ACS Earth Space Chem.* **2019,** *3*, (10), 2225-2236.
(28) Yin, H.; Wu, Y.; Hou, J.; Yan, X.; Li, Z.; Zhu, C.; Zhang, J.; Feng, X.; Tan, W.; Liu, F. Preference of Co over Al for substitution of Fe in goethite (α-FeOOH) structure: Mechanism revealed from EXAFS, XPS, DFT and linear free energy correlation model. *Chem. Geol.* **2020,** *532*, 119378.
(29) Guinoiseau, D.; Gélabert, A.; Moureau, J.; Louvat, P.; Benedetti, M. F. Zn isotope fractionation during sorption onto kaolinite. *Environ. Sci. Technol.* **2016,** *50*, (4), 1844-1852.
(30) Mo, X.; Siebecker, M. G.; Gou, W.; Li, L.; Li, W. A review of cadmium sorption mechanisms on soil mineral surfaces revealed from synchrotron-based X-ray absorption fine structure spectroscopy: Implications for soil remediation. *Pedosphere* **2021,** *31*, (1), 11-27.
(31) Bryan, A. L.; Dong, S.; Wilkes, E. B.; Wasylenki, L. E. Zinc isotope fractionation during adsorption onto Mn oxyhydroxide at low and high ionic strength. *Geochim. Cosmochim. Acta* **2015,** *157*, 182-197.
(32) Mavromatis, V.; González, A. G.; Dietzel, M.; Schott, J. Zinc isotope fractionation during the inorganic precipitation of calcite – Towards a new pH proxy. *Geochim. Cosmochim. Acta* **2019,** *244*, 99-112.
(33) DePaolo, D. J. Surface kinetic model for isotopic and trace element fractionation during precipitation of calcite from aqueous solutions. *Geochim. Cosmochim. Acta* **2011,** *75*, (4), 1039-1056.
(34) Xie, X.; Yan, L.; Li, J.; Guan, L.; Chi, Z. Cadmium isotope fractionation during Cd-calcite coprecipitation: Insight from batch experiment. *Sci. Total Environ.* **2021,** *760*, 143330.
(35) Schauble, E. A. Applying stable isotope fractionation theory to new systems. *Rev. Mineral. Geochem.* **2004,** *55*, (1), 65-111.
(36) Little, S. H.; Sherman, D. M.; Vance, D.; Hein, J. R. Molecular controls on Cu and Zn isotopic fractionation in Fe-Mn crusts. *Earth Planet. Sci. Lett.* **2014,** *396*, 213-222.
(37) Fujii, T.; Moynier, F.; Telouk, P.; Abe, M. Experimental and theoretical investigation of isotope fractionation of zinc between aqua, chloro, and macrocyclic complexes. *J. Phys. Chem. A* **2010,** *114*, (7), 2543-2552.
(38) Fujii, T.; Moynier, F.; Dauphas, N.; Abe, M. Theoretical and experimental investigation of nickel isotopic fractionation in species relevant to modern and ancient oceans. *Geochim. Cosmochim. Acta* **2011,** *75*, (2), 469-482.
(39) Fujii, T.; Moynier, F.; Blichert-Toft, J.; Albarède, F. Density functional theory estimation of isotope fractionation of Fe, Ni, Cu, and Zn among species relevant to geochemical and biological environments. *Geochim. Cosmochim. Acta* **2014,** *140*, 553-576.
(40) Yin, H.; Tan, N.; Liu, C.; Wang, J.; Liang, X.; Qu, M.; Feng, X.; Qiu, G.; Tan, W.; Liu, F. The associations of heavy metals with crystalline iron oxides in the polluted soils around the mining areas in Guangdong Province, China. *Chemosphere* **2016,** *161*, 181-189.
(41) Cornell, R. M.; Schwertmann, U. *The iron oxides : structure, properties, reactions,*

659 *occurences and uses*. Wiley-VCH: Weinheim, 2003.
660 (42) Speight, J. G. *Lange's handbook of chemistry*. Sixteenth ed.; MCGRAW-HILL:
661 Wyoming, 2005.
662 (43) Zhang, Y.; Wen, H.; Zhu, C.; Fan, H.; Cloquet, C. Cadmium isotopic evidence for
663 the evolution of marine primary productivity and the biological extinction event during
664 the Permian-Triassic crisis from the Meishan section, South China. *Chem. Geol.* **2018,**
665 *481*, 110-118.
666 (44) Zhu, C.; Wen, H.; Zhang, Y.; Fan, H.; Fu, S.; Xu, J.; Qin, T. Characteristics of Cd
667 isotopic compositions and their genetic significance in the lead-zinc deposits of SW
668 China. *Sci. China Earth Sci.* **2013,** *56*, (12), 2056-2065.
669 (45) Cloquet, C.; Rouxel, O.; Carignan, J.; Libourel, G. Natural cadmium isotopic
670 variations in eight geological reference materials (NIST SRM 2711, BCR 176, GSS-1,
671 GXR-1, GXR-2, GSD-12, Nod-P-1, Nod-A-1) and anthropogenic samples, measured
672 by MC-ICP-MS. *Geostand. Geoanal. Res.* **2005,** *29*, (1), 95-106.
673 (46) Zhang, Y.; Wen, H.; Zhu, C.; Fan, H.; Luo, C.; Liu, J.; Cloquet, C. Cd isotope
674 fractionation during simulated and natural weathering. *Environ. Pollut.* **2016,** *216*, 9-
675 17.
676 (47) Ravel, B.; Newville, M. ATHENA, ARTEMIS, HEPHAESTUS: data analysis for
677 X-ray absorption spectroscopy using IFEFFIT. *J. Synchrotron Radiat.* **2005,** *12*, (Pt 4),
678 537-41.
679 (48) Kelly, S. D.; Hesterberg, D.; Ravel, B. Analysis of soils and minerals using X-ray
680 absorption spectroscopy. In *Methods of Soil Analysis, Part 5-MineralogicalMethods*,
681 Ulrey, A. L.; Drees, R. L., Eds. Soil Science Society of America.: 2008.
682 (49) Rehr, J. J.; Albers, R. C.; Zabinsky, S. I. High-order multiple-scattering calculations
683 of x-ray-absorption fine structure. *Phys. Rev. Lett.* **1992,** *69*, (23), 3397-3400.
684 (50) Sun, Q.; Cui, P.-X.; Zhu, M.; Fan, T.-T.; Ata-Ul-Karim, S. T.; Gu, J.-H.; Wu, S.;
685 Zhou, D.-M.; Wang, Y.-J. Cd(II) retention and remobilization on δ-MnO_2 and Mn(III)-
686 rich δ-MnO_2 affected by Mn(II). *Environ. Int.* **2019,** *130*, 104932.
687 (51) Teo, B. K. *EXAFS: Basic Principles and Data Analysis*. Springer Berlin Heidelberg:
688 2012.
689 (52) Bochatay, L.; Persson, P.; Sjöberg, S. Metal ion coordination at the water–
690 manganite (γ-MnOOH) interface: I. An EXAFS study of cadmium(II). *J. Colloid*
691 *Interface Sci.* **2000,** *229*, (2), 584-592.
692 (53) Rout, K.; Mohapatra, M.; Anand, S. 2-line ferrihydrite: synthesis, characterization
693 and its adsorption behaviour for removal of Pb(II), Cd(II), Cu(II) and Zn(II) from
694 aqueous solutions. *Dalton Trans.* **2012,** *41*, (11), 3302-12.
695 (54) Jiang, W.; Lv, J.; Luo, L.; Yang, K.; Lin, Y.; Hu, F.; Zhang, J.; Zhang, S. Arsenate
696 and cadmium co-adsorption and co-precipitation on goethite. *J. Hazard. Mater.* **2013,**
697 *262*, 55-63.
698 (55) Li, W.; Zhang, S.; Jiang, W.; Shan, X. Q., Effect of phosphate on the adsorption of
699 Cu and Cd on natural hematite. *Chemosphere* **2006,** *63*, (8), 1235-41.
700 (56) Boyanov, M. I.; Kelly, S. D.; Kemner, K. M.; Bunker, B. A.; Fein, J. B.; Fowle, D.
701 A., Adsorption of cadmium to Bacillus subtilis bacterial cell walls: a pH-dependent X-

ray absorption fine structure spectroscopy study. *Geochim. Cosmochim. Acta* **2003,** *67*, (18), 3299-3311.
(57) Gräfe, M.; Mustafa, G.; Singh, B.; Kookana, R. S. Chapter 7 Temperature and Aging Effects on the Surface Speciation of Cd(II) at the Goethite–Water Interface. In *Developments in Earth and Environmental Sciences*, Barnett, M. O.; Kent, D. B., Eds. Elsevier: 2007; Vol. 7, pp 187-204.
(58) Rietveld, H. M. A profile refinement method for nuclear and magnetic structures. *J. Appl. Crystallogr.* **1969,** *2*, (2), 65-71.
(59) Huynh, T.; Tong, A. R.; Singh, B.; Kennedy, B. J. Cd-substituted goethites - A structural investigation by synchrotron X-ray diffraction. *Clays Clay Miner.* **2003,** *51*, (4), 397-402.
(60) Kaur, N.; Gräfe, M.; Singh, B.; Kennedy, B., Simultaneous incorporation of Cr, Zn, Cd, and Pb in the goethite structure. *Clays Clay Miner.* **2009,** *57*, (2), 234-250.
(61) Pokrovsky, O. S.; Viers, J.; Emnova, E. E.; Kompantseva, E. I.; Freydier, R. Copper isotope fractionation during its interaction with soil and aquatic microorganisms and metal oxy(hydr)oxides: Possible structural control. *Geochim. Cosmochim. Acta* **2008,** *72*, (7), 1742-1757.
(62) Wilkins, R. G. Mechanisms of ligand replacement in octahedral nickel(II) complexes. *Acc. Chem. Res.* **1970,** *3*, (12), 408-416.
(63) Wilkins, R. G. *Kinetics and Mechanism of Reactions of Transition Metal Complexes*. Wiley: 1991.
(64) Randall, S. R.; Sherman, D. M.; Ragnarsdottir, K. V.; Collins, C. R. The mechanism of cadmium surface complexation on iron oxyhydroxide minerals. *Geochim. Cosmochim. Acta* **1999,** *63*, (19), 2971-2987.
(65) Boily, J. F.; Sjoberg, S.; Persson, P. Structures and stabilities of Cd(II) and Cd(II)-phthalate complexes at the goethite/water interface. *Geochim. Cosmochim. Acta* **2005,** *69*, (13), 3219-3235.
(66) Collins, C. R.; Ragnarsdottir, K. V.; Sherman, D. M. Effect of inorganic and organic ligands on the mechanism of cadmium sorption to goethite. *Geochim. Cosmochim. Acta* **1999,** *63*, (19), 2989-3002.
(67) Barrón, V.; Torrent, J. Surface hydroxyl configuration of various crystal faces of hematite and goethite. *J. Colloid Interface Sci.* **1996,** *177*, (2), 407-410.
(68) Villalobos, M.; Cheney, M. A.; Alcaraz-Cienfuegos, J. Goethite surface reactivity: II. A microscopic site-density model that describes its surface area-normalized variability. *J. Colloid Interface Sci.* **2009,** *336*, (2), 412-422.
(69) Venema, P.; Hiemstra, T.; Weidler, P. G.; van Riemsdijk, W. H. Intrinsic proton affinity of reactive surface groups of metal (hydr)oxides: Application to iron (hydr)oxides. *J. Colloid Interface Sci.* **1998,** *198*, (2), 282-295.
(70) Gustafsson, J. P. Visual MINTEQ 3.1； KTH (Royal Institute of Technology): Stockholm, Sweden. **2014**.
(71) Sheng, A.; Liu, J.; Li, X.; Qafoku, O.; Collins, R. N.; Jones, A. M.; Pearce, C. I.; Wang, C.; Ni, J.; Lu, A.; Rosso, K. M. Labile Fe(III) from sorbed Fe(II) oxidation is the key intermediate in Fe(II)-catalyzed ferrihydrite transformation. *Geochim. Cosmochim.*

Acta **2020,** *272*, 105-120.
(72) Sheng, A.; Li, X.; Arai, Y.; Ding, Y.; Rosso, K. M.; Liu, J. Citrate controls Fe(II)-catalyzed transformation of ferrihydrite by complexation of the labile Fe(III) intermediate. *Environ. Sci. Technol.* **2020,** *54*, (12), 7309-7319.
(73) Clayton, R. E.; Hudson-Edwards, K. A.; Malinovsky, D.; Andersson, P. Fe isotope fractionation during the precipitation of ferrihydrite and transformation of ferrihydrite to goethite. *Mineral. Mag.* **2005,** *69*, (5), 667-676.
(74) Guinoiseau, D.; Galer, S. J. G.; Abouchami, W.; Frank, M.; Achterberg, E. P.; Haug, G. H. Importance of cadmium sulfides for biogeochemical cycling of Cd and its isotopes in oxygen deficient zones—A case study of the Angola Basin. *Global Biogeochem. Cy.* **2019,** *33*, (12), 1746-1763.
(75) Cloquet, C.; Carignan, J.; Libourel, G.; Sterckeman, T.; Perdrix, E. Tracing source pollution in soils using cadmium and lead isotopes. *Environ. Sci. Technol.* **2006,** *40*, (8), 2525-2530.
(76) Wiggenhauser, M.; Bigalke, M.; Imseng, M.; Muller, M.; Keller, A.; Murphy, K.; Kreissig, K.; Rehkamper, M.; Wilcke, W.; Frossard, E. Cadmium isotope fractionation in soil-wheat systems. *Environ. Sci. Technol.* **2016,** *50*, (17), 9223-9231.
(77) Zhong, Q.; Zhou, Y.; Tsang, D. C. W.; Liu, J.; Yang, X.; Yin, M.; Wu, S.; Wang, J.; Xiao, T.; Zhang, Z. Cadmium isotopes as tracers in environmental studies: A review. *Sci. Total Environ.* **2020,** *736*, 139585.

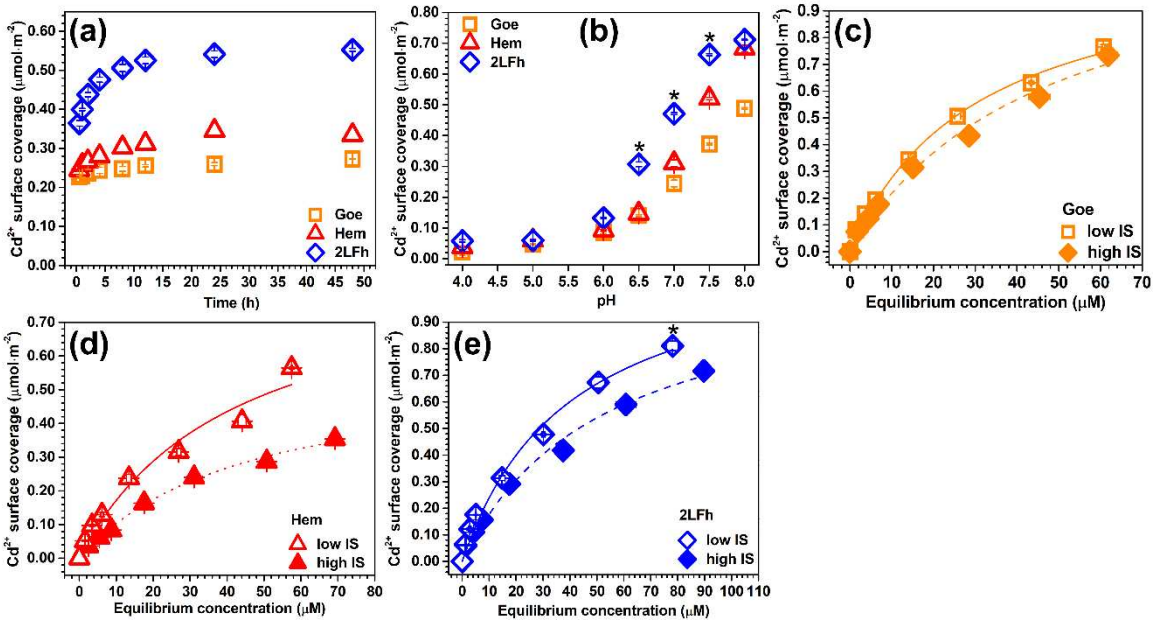

772

773 **Fig. 1** Macroscopic adsorption behavior of Cd^{2+} on Goe, Hem and 2LFh under different
774 reaction conditions. (a) Adsorption kinetics at pH 7 ± 0.05 with a duration time of 48
775 h. (b) Sorption edges. The Cd initial concentrations ($[Cd^{2+}]$) were set as 22.2 μM, 44.5
776 μM and 89.0 μM for Goe, Hem and 2LFh, respectively, in both kinetics and sorption
777 edges experiments, with background electrolyte of 0.05 M KNO_3 solution. Adsorption
778 isotherm curves at low and high ionic strength (IS: 0.05 M and 0.36 M KNO_3 solution)
779 at pH 7 ± 0.05 for (c) Goe, (d) Hem, and (e) 2LFh, with $[Cd^{2+}]$ = 0-89.0 μM for Goe,
780 Hem and $[Cd^{2+}]$ = 0-177.9 μM for 2LFh. Symbols are experimental data, and lines are
781 Langmuir fits. All experiments were conducted using a solid/solution ratio of 1 $g \cdot L^{-1}$
782 for Goe and Hem, and 0.5 $g \cdot L^{-1}$ for 2LFh at 25 ± 2 °C. In panels (b) and (e), the samples
783 indicated by asterisk (*) were selected for Cd K-edge EXAFS analysis.

784

785

786

787

788

789

790

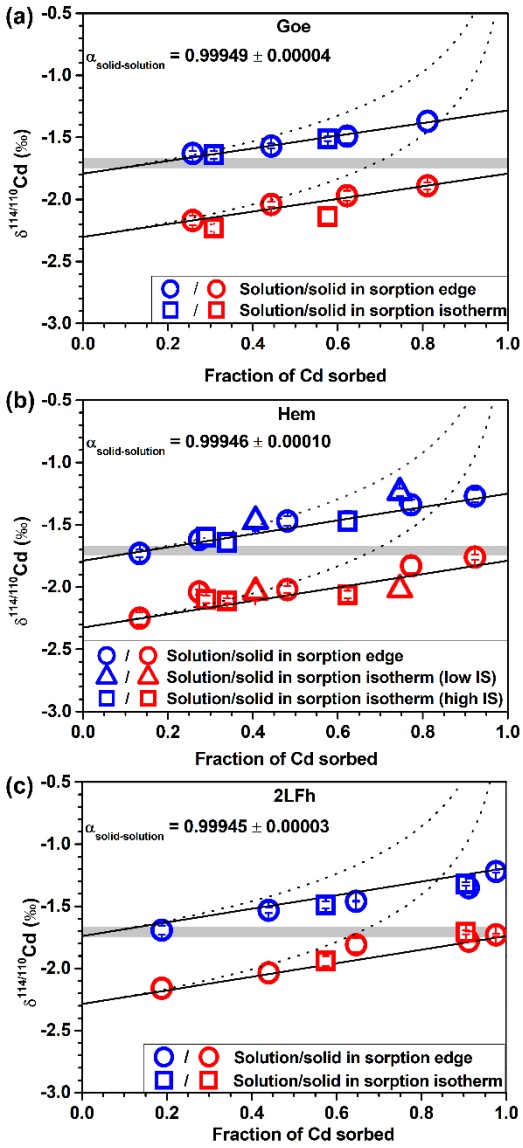

Fig. 2 The Cd isotope compositions between solution and solid phases as the function of Cd adsorbed fraction during adsorption onto Goe (a), Hem (b) and 2LFh (c). The solid lines and dashed curves represent the theoretical $\delta^{114/110}$Cd values calculated using the equilibrium model and the Rayleigh model, respectively. The fractionation factor ($\alpha_{solid\text{-}solution}$) given is the average of the two values determined using $\delta^{114/110}$Cd in solution and in solid separately using the equilibrium model. The Cd^{2+} stock solution used for adsorption experiments has a $\delta^{114/110}$Cd value of -1.71 ± 0.04‰ (gray line in each panel).

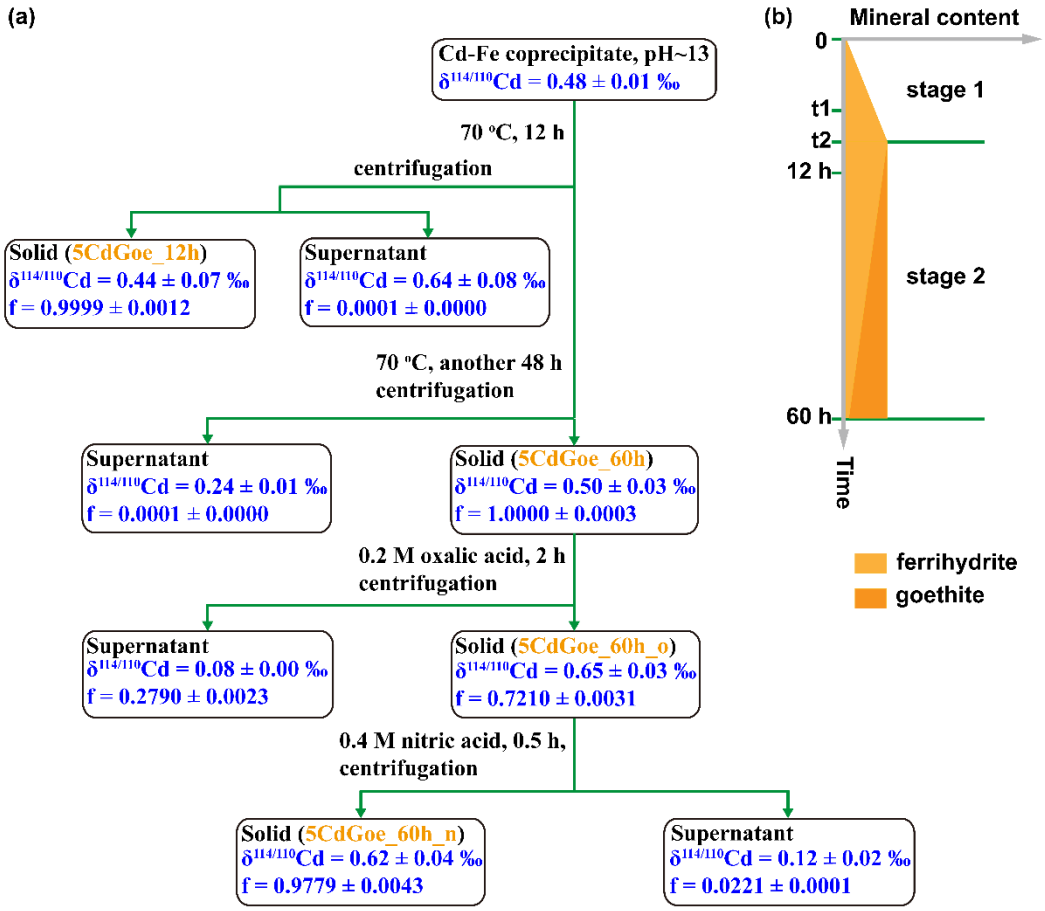

801

802 **Fig. 3** (a) An illustration of Cd isotope mass balance during Cd-doped goethite
803 synthesis. Cadmium isotope composition and the fraction of Cd (f) in each part were
804 added. (b) The corresponding changes in the contents of ferrihydrite and goethite with
805 time. Time t1 refers to the time that the kinetic isotope fractionation of Cd was removed,
806 while t2 refers to the time that the ferrihydrite crystallization was completed.

807

Table 1. Fitting results of EXAFS spectra for model compounds and typical Cd adsorption and coprecipitation samples, including in the fit of the first Cd-O coordination shell a third cumulant (cum.) to account for the asymmetry in a non-Gaussian model.

Sample	Path	CN	R (Å)	σ^2 (Å^2)	Third cum.	ΔE (eV)	χ^2	R-factor[a]
$Cd(NO_3)_2$	Cd-O	6.6 ± 0.6	2.29 ± 0.02 (2.27 ± 0.01)[b]	0.0086 ± 0.0010	0.0003 ± 0.0004	3.3 ± 1.7	41.82	0.0058
$Cd(OH)_2$[c]	Cd-O	7.4 ± 1.1	2.31 ± 0.02 (2.30 ± 0.01)	0.0090 ± 0.0018	0.0004 ± 0.0005	6.5 ± 1.4	3510.01	0.0177
	Cd-Cd	10.2 ± 2.7	3.51 ± 0.01	0.0117 ± 0.0021				
CdFh_10_pH6.5[d]	Cd-O	6.2 ± 0.7	2.30 ± 0.03 (2.24 ± 0.01)	0.0118 ± 0.0014	0.0011 ± 0.0006	2.4 ± 2.1	2.00	0.0119
	Cd-Fe	0.7 ± 0.4	3.31 ± 0.02	0.0029 ± 0.0047				
CdFh_10_pH7[d]	Cd-O	7.4 ± 1.0	2.31 ± 0.04 (2.26 ± 0.01)	0.0143 ± 0.0020	0.0010 ± 0.0008	4.1 ± 2.4	45.89	0.0195
	Cd-Fe	4.7 ± 1.3	3.33 ± 0.05	0.0282 ± 0.0165				
CdFh_20_pH7[d]	Cd-O	5.7 ± 1.2	2.28 ± 0.05 (2.24 ± 0.01)	0.0086 ± 0.0024	0.0007 ± 0.0009	3.2 ± 3.9	22.62	0.0482
	Cd-Fe	0.7 ± 0.3	3.33 ± 0.04	0.0030[e]				
CdFh_10_pH7.5[d]	Cd-O	5.8 ± 0.7	2.32 ± 0.03 (2.26 ± 0.01)	0.0106 ± 0.0014	0.0011 ± 0.0006	5.2 ± 2.1	18.82	0.0139
	Cd-Fe	0.8 ± 1.0	3.36 ± 0.03	0.0097 ± 0.0101				
5CdGoe_60h_n	Cd-O	6.4 ± 1.6	2.29 ± 0.06 (2.22 ± 0.02)	0.0085 ± 0.0031	0.0013 ± 0.0012	7.6 ± 4.4	56.20	0.0675
	Cd-Fe	0.4 ± 0.9	3.07 ± 0.04	0.0004±0.0168				

[a]R indicates the fitting quality, which is calculated by the equation: $R = \sum(k^2\chi_{obs}(k) - k^2\chi_{cal}(k))^2/\sum(k^2\chi_{obs}(k))^2$.

[b]These values in bracket were those derived from first Cd-O shell fitting without the addition of third cumulant.

[c]This standard was adopted from our previous study[27].

[d]These samples were named as CdMineral _initial Cd concentration_reaction pH, and the isotope compositions of these samples were measured.

[e]This parameter was fixed during the fitting.

817 **TOC**

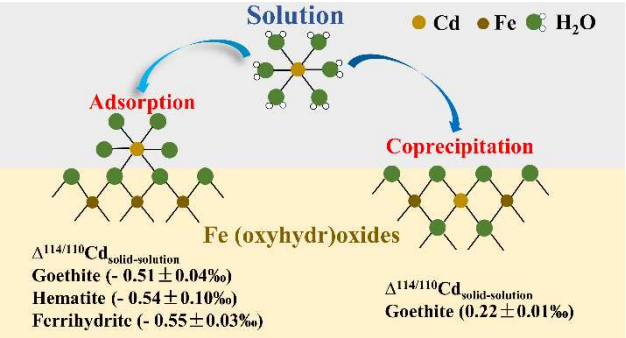

818

819

820

821

822

823